HHS Public Access

Author manuscript

Acta Biomater. Author manuscript; available in PMC 2020 November 08.

Published in final edited form as:

Acta Biomater. 2018 April 15; 71: 37–48. doi:10.1016/j.actbio.2018.02.026.

The *in vitro* effects of macrophages on the osteogenic capabilities of MC3T3-E1 cells encapsulated in a biomimetic poly(ethylene glycol) hydrogel

Leila S. Saleh[a], **Maria Carles-Carner**[a], **Stephanie J. Bryant**[a,b,c,*]

[a]Department of Chemical and Biological Engineering, University of Colorado, 3415 Colorado Avenue, Boulder, CO 80303, USA

[b]BioFrontiers Institute, University of Colorado, 3415 Colorado Avenue, Boulder, CO 80303, USA

[c]Material Science and Engineering Program, University of Colorado, 3415 Colorado Avenue, Boulder, CO 80303, USA

Abstract

Poly(ethylene glycol) PEG-based hydrogels are promising for cell encapsulation and tissue engineering, but are known to elicit a foreign body response (FBR) *in vivo*. The goal of this study was to investigate the impact of the FBR, and specifically the presence of inflammatory macrophages, on encapsulated cells and their ability to synthesize new extracellular matrix. This study employed an *in vitro* co-culture system with murine macrophages and MC3T3-E1 pre-osteoblasts encapsulated in a bone-mimetic hydrogel, which were cultured in transwell inserts, and exposed to an inflammatory stimulant, lipopolysaccharide (LPS). The co-culture was compared to mono-cultures of the cell-laden hydrogels alone and with LPS over 28 days. Two macrophage cell sources, RAW 264.7 and primary derived, were investigated. The presence of LPS-stimulated primary macrophages led to significant changes in the cell-laden hydrogel by a 5.3-fold increase in percent apoptotic osteoblasts at day 28, 4.2-fold decrease in alkaline phosphatase activity at day 10, and 7-fold decrease in collagen deposition. The presence of LPS-stimulated RAW macrophages led to significance changes in the cell-laden hydrogel by 5-fold decrease in alkaline phosphatase activity at day 10 and 4-fold decrease in collagen deposition. Mineralization, as measured by von Kossa stain or quantified by calcium content, was not sensitive to macrophages or LPS. Elevated interleukin-6 and tumor necrosis factor-α secretion were detected in mono-cultures with LPS and co-cultures. Overall, primary macrophages had a more severe inhibitory effect on osteoblast differentiation than the macrophage cell line, with greater apoptosis and collagen I reduction. In summary, this study highlights the detrimental effects of macrophages on encapsulated cells for bone tissue engineering.

Keywords

Poly(ethylene glycol) hydrogel; macrophage; MC3T3-E1 pre-osteoblast; co-culture; host response; osteogenesis

*Corresponding Author.

1. Introduction

Synthetic hydrogels with their high water content are promising platforms to encapsulate cells in three-dimensional (3D) scaffolds for tissue engineering. Moreover, extracellular matrix (ECM) moieties and degradable crosslinks are readily incorporated into synthetic hydrogels creating highly tunable 3D environments that can be designed to direct cell fate and promote tissue growth [1–6]. Injection and/or implantation of cell-laden hydrogels has several benefits over *ex vivo* tissue engineering. These benefits include the presence of local cues that are native to the tissue environment, improved integration of the engineered tissue with the host tissue, and removing the need for long-term culture prior to implantation. However, the *in vivo* environment introduces additional complexities, which may affect the ability of cells to synthesize and deposit tissue. While numerous studies have focused on hydrogel designs to promote growth of a specific tissue, the impact of the *in vivo* environment is not well understood. This environment, however, will be critical to the *in vivo* translation of a tissue engineering strategy.

When any cell-laden scaffold is placed *in vivo*, the process of surgically implanting the scaffold injures the surrounding tissue and induces an acute inflammatory response. For non-biological scaffolds, this response will lead to a sustained foreign body response (FBR). The FBR is a localized innate immune response [7], beginning with immediate non-specific protein adsorption and resolving in the characteristic persistent presence of macrophages, chronic inflammation, and fibrous encapsulation [8]. The FBR occurs ubiquitously to nearly all non-biological materials [9] and is considered a normal, biocompatible response to implanted scaffolds [10]. More specifically, a FBR marked by fibrosis and prolonged inflammation has been reported to a wide range of implanted hydrogels that include crosslinked collagen hydrogels [11], dextran-based hydrogels [12], alginate hydrogels [13], poly(2-hydroxyethyl methacrylate) hydrogels [10], poly(ethylene glycol) hydrogels [14,15], poly(lactic acid-*b*-ethylene glycol-*b*-lactic acid) hydrogels [16], PEG/sebacic acid-based hydrogels [15], and poly(propylene fumarate-co-ethylene glycol) [17]. Though often considered non-fouling due to their hydrophilicity, PEG surfaces have been shown to readily adsorb proteins [18]. We have extensively characterized the FBR to PEG hydrogels and reported that *in vitro* macrophages readily attach to PEG hydrogels through non-specific protein adsorption and that *in vivo* macrophages are recruited to the implant site within two days post-implantation [19–22] and a fibrous capsule forms within four weeks [23]. While the FBR to hydrogels has been studied extensively, the impact of the FBR on cell-laden hydrogels has received less attention.

Although many implants (e.g., arterial stents, artificial joints) can function despite the FBR, tissue engineering strategies, where cells are delivered within the scaffold, require that the cells themselves function to synthesize and deposit their own tissue. Several studies have indicated that the events associated with the FBR may have negative consequences for tissue engineering. For example, we previously reported that inflammatory macrophages seeded directly on top of a PEG hydrogel with encapsulated fibroblasts adversely affected the fibroblasts by reducing gene expression of ECM molecules and elevating gene expression for pro-inflammatory cytokines [24]. In another study, a distinct FBR was noted with increased macrophage presence concomitant with diminished cartilage regeneration when a

cell-laden poly(l-lactic acid) scaffold was placed into a cartilage defect of a canine model [25]. In addition, the presence of a fibrous capsule created a barrier between an oligo(poly(ethylene glycol) fumarate) hydrogel that was implanted into a rabbit cranial bone defect and newly formed bone at the perimeter of the defect [26]. Collectively, these studies and others demonstrate that the events associated with the FBR can impede tissue regeneration and integration for implanted scaffolds, thus warranting further study.

The overall goal for this study was to examine the effects of macrophages, the drivers of chronic inflammation in the FBR, on the long-term culture of a cell-laden hydrogel for bone tissue engineering. To achieve this goal, an *in vitro* co-culture model system was used. MC3T3-E1 pre-osteoblastic cells were encapsulated in a degradable bone mimetic hydrogel and cultured in a transwell configuration in the presence of murine macrophages. This model enabled paracrine signaling between MC3T3-E1 cells and macrophages to be investigated. A photoclickable and degradable PEG hydrogel based on the thiol and norbornene click reaction was chosen for its promise in tissue engineering [27,28] and for its ease with which ECM moieties are introduced via the click chemistry [29–32]. Herein, MC3T3-E1 cells were encapsulated in a bone mimetic hydrogel containing the cell-adhesion peptide, RGD, matrix metalloproteinase (MMP)-sensitive peptide crosslinks, and hydroxyapatite particles. Moreover, we have previously confirmed the FBR to MMP-sensitive PEG hydrogels with the accumulation of inflammatory cells and fibrous encapsulation in a subcutaneous mouse model over the course of four weeks [21].

The specific objective of this study was to evaluate the cell-laden hydrogels for cell apoptosis, cellular morphology, osteogenic capabilities, and ECM deposition under *in vitro* simulated FBR conditions by two different macrophage sources. Macrophages (i.e. a murine macrophage cell line (RAW 264.7) and macrophages derived from murine bone marrow monocytes [33]), have been shown to differ in their activation *in vitro* [34] and therefore could differentially affect the cell-laden hydrogels. We hypothesized that classically activated macrophages will inhibit osteogenesis and ECM synthesis of the encapsulated pre-osteoblasts. Additionally, due to their higher pro-inflammatory cytokine activity [35,36], we further hypothesize that primary macrophages will have a more pronounced inhibitory effect on the encapsulated pre-osteoblasts when compared to the RAW 264.7 macrophages. Hydrogels were subjected to prolonged exposure to induce classically activated macrophages and simulate the paracrine signals resulting from the persistent macrophage presence at the implant site *in vivo.* Findings from this study demonstrate that while MC3T3-E1 cells are able to secrete bone-like ECM molecules within the bone mimetic hydrogel, osteogenic capabilities and ECM accumulation are compromised under simulated FBR conditions, but in a manner that depends on the macrophage source. Findings from this study further support the idea that the macrophages associated with the FBR can impede tissue growth in cell-laden synthetic-based hydrogels.

2. Materials and Methods

2.1. Macromer synthesis and hydrogel formation

The macromolecular monomer (macromer), 8-arm poly(ethylene glycol) functionalized with norbornene, was synthesized following established protocols [29,31]. Briefly, 8-arm PEG-

NH_2 (20 kDa, JenKemUSA) was dissolved in dimethylformamide (Sigma) and reacted overnight with excess 5-norbornene-2-carboxylic acid (Sigma), 2-(1H-7-Azabenzotriazol-1-yl)1,1,3,3-tetramethyl uronium hexafluorophosphate methanaminium (Sigma), and N,N-Di-isopropylethylamine (Sigma). The product was precipitated in cold diethyl ether, dialyzed against de-ionized water, and lyophilized. Functionalization of each arm of a PEG molecule with a norbornene was confirmed to be >95% by ^{1}H-NMR.

A precursor solution was prepared with 8% (w/w) 8-arm PEG norbornene, 2.5 mM CRGDS (Genscript), the bis-cysteine MMP sensitive crosslinker GCVPLS-LYSGCG (Genscript), which has been shown to be sensitive to MMP-2 [21], at a 0.83 [thiol]:[ene] molar ratio for the crosslinker to the 8-arm macromer, and 0.05% (w/w) photoinitiator (Irgacure 2959, BASF) in phosphate buffered saline (PBS, pH 7.4). The precursor solution was sterile filtered (0.22 μm). Hydroxyapatite nanoparticles (HA, Sigma) were sterilized by autoclave and then combined with the precursor solution at 1% (w/w). This precursor solution was well mixed and polymerized immediately under 352 nm light at 6 mW/cm^2 for 6 minutes in cylindrical molds of ~2 mm height and 4.5 mm diameter. There were no observable signs of hydroxyapatite nanoparticle settling. All procedures were performed in a biosafety cabinet following aseptic techniques with sterilized instruments.

2.2 Raman Spectroscopy

Acellular hydrogels containing 0 or 1% (w/w) hydroxyapatite nanoparticles were lyophilized and Raman spectra were collected using a Horiba LabRAM HR Evolution Raman spectrometer. The spectrometer was calibrated using the 520 cm-1 Raman peak of Si. A spatial resolution of ~2μm and 29 mW power at the sample surface were achieved by 532nm laser beam focused through a 50x L WD (0.75 NA) objective lens. Spectral resolution of 4.5 cm-1 full width at half maximum was achieved by a 600 lines/mm grating with 100 μm confocal pinhole. Spectra are displayed as an average of 15 accumulated spectra collected with a 2 second counting time. Instrumental artifacts were corrected for and a polynomial baseline was subtracted using LabSpec 6 (Horiba Scientific). The spectroscopy work was performed at the Raman Microspectroscopy Lab at the University of Colorado Boulder.

2.3 Characterization of the acellular hydrogel

Acellular hydrogels containing 0 or 1% (w/w) hydroxyapatite nanoparticles were collected and assessed for compressive modulus and wet and dry weights. Hydrogels were compressed to 15% strain at 0.5 mm/min by a mechanical tester (MTS Synergie 100) with a 10 N load cell. Compressive modulus was determined by the slope of the linear region between 10 and 15% strain on the stress-strain curve. Wet weights were measured before lyophilization and dry weights were measured after lyophilization. The equilibrium mass swelling ratio was defined as the wet weight divided by the dry weight. The equilibrium volumetric ratio was determined from the mass swelling ratio, the solvent density assuming 1 g/mL and the polymer density assuming 1.07 g/mL. Hydrogel mesh size was estimated from Flory-Rehner theory and methods described by Canal and Peppas [37] using polymer-solvent interaction parameter described in [38]. Hydroxyapatite nanoparticles were assessed for their size by field emission scanning electron microscopy (FESEM, JEOL JSM-7401F).

Briefly, a 1 mg/mL solution of HA nanoparticles in diH_20 was dried, sputter coated with a thin layer of gold (thickness ~ 3–5 nm) and examined. NIH Image J was used to ascertain particle diameter.

2.4 MC3T3-E1 cell culture and encapsulation

A murine pre-osteoblast cell line MC3T3-E1 (ATCC, CRL-2593) was expanded in alpha-MEM media (Gibco) with 10% fetal bovine serum (FBS, Atlanta Biologicals) and 50 U/mL penicillin, 50 μg/mL streptomycin (1% P/S, Corning). MC3T3-E1 cells were cultured to ~90% confluency and then collected using 0.05% trypsin/EDTA (Gibco). Cells were combined at 2×10^7 cells per mL precursor solution and polymerized as described above. Cell-laden hydrogels were cultured in 24-well plates as mono-cultures or in a 24-well transwell inserts with RAW 264.7 or primary murine macrophages (see below) seeded at the bottom of the well plates as co-cultures. The mono-culture and co-cultures were placed in osteogenic differentiation media containing alpha-MEM, 10% FBS, 1% P/S, supplemented with 10 mM β-glycerophosphate (Sigma), 0.1 mM dexamethasone (Sigma), and 50 μg/ml L-Ascorbic acid 2-phosphate sesquimagnesium salt hydrate (Sigma). The medium was supplemented or not with 1 μg/mL lipopolysaccharide from *E. coli* (LPS-EB O111:B4, standard purity, Invitrogen).

2.5 RAW 264.7 cell culture

A murine macrophage cell line RAW 264.7 (ATCC, TIB-71) was expanded in DMEM (Gibco) supplemented with 10% FBS (Atlanta Biologicals) and 1% P/S (Corning) with 0.05% Fungizone (Corning). RAW 264.7 cells were cultured to ~85% confluency and then collected using a cell scraper. Macrophages were plated at 2,650 cells/cm^2 in the bottom of 24 well plates and allowed to adhere overnight. At which time, MC3T3-E1-laden hydrogels were placed into the wells containing macrophages using transwell inserts. The co-culture system was then cultured in osteogenic differentiation medium with or without LPS as described above and medium exchanged every two days. Weekly, macrophages were refreshed by plating new macrophages in a 24 well plate following methods just described and transferring the MC3T3-E1-laden hydrogels along with the transwell inserts to the new 24 well plates.

2.6 Primary monocyte isolation, differentiation, and culture

Bone marrow derived monocytes were isolated following established protocols [33] from the long bones of 6–8 week old C57BL/6 mice (Charles River Laboratories) by flushing and collecting the bone marrow with Iscove's Modified Dulbecco's Mediu9m (IMDM, Gibco) containing 10% FBS, 1% P/S, and 0.5% Fungizone layered with Lympholyte M (CedarLane). Mononuclear cells were plated on non-tissue culture treated polystyrene and differentiated for 10 days in media containing IMDM, 20% FBS, 1% P/S, 0.5% Fungizone, 2 mM L-Glutamine, 1.5 ng/mL human macrophage colony stimulating factor (hMCSF, R&D Systems), and 100 ng/mL huFLT-3 (R&D Systems). After differentiation, cells were collected by a cell scraper and plated at 2,650 cells/cm^2 in the bottom of 24 well plates and allowed to adhere overnight. At which time, MC3T3-E1-laden hydrogels were placed in transwell inserts and into the 24 well plates with macrophages. Following the same methods described above for RAW 264.7 macrophages, the co-culture system was cultured in

osteogenic differentiation medium with or without LPS. Freshly isolated and differentiated primary macrophages were refreshed weekly. Medium was refreshed every two days.

2.7 Assessment of MC3T3-E1 pre-osteoblast morphology

Cell morphology was visualized by live cellular staining with 4 nM calcein AM (Corning) immediately after encapsulation and after 10 days of culture in the mono-cultures and co-cultures. Whole gels (n = 3–4) were cut in half and the cross-section, interior side was imaged by laser scanning confocal microscopy (Zeiss LSM 150).

2.8 Immunohistochemical and histological analysis

For immunohistochemical and histological analysis, MC3T3-E1-laden hydrogels (n = 3–4) were collected at days 0 (i.e., one day after encapsulation), 10, and 28 and fixed in neutral-buffered formalin for four hours at room temperature, then dehydrated and embedded in paraffin following standard protocols. Sections (10 μm) were deparaffinized, hydrated, and stained for apoptosis, anti-collagen I, or mineralization. Sections were stained for apoptotic cells using the DeadEnd Fluorometric TUNEL system (Promega) per manufacturer instructions. Sections were counterstained with DAPI for nuclei. Sections were imaged by laser scanning confocal microscopy where apoptotic cells were indicated by green fluorescence and nuclei indicated by blue fluorescence. Four images per hydrogel were acquired per hydrogel and total nuclei and the number of positively stained apoptotic cells were counted per image using NIH Image J and the average percent apoptotic cells per hydrogel was determined. For anti-collagen I, sections were pretreated with 1 mg/mL pepsin (Sigma) followed by antigen retrieval (Retrievagen, BD Biosciences). After permeabilization and blocking, sections were incubated with collagen I antibody (1:50, Abcam, ab34710) in blocking solution overnight at 4°C. Sections were then treated with a secondary antibody, AlexaFluor 546 goat anti-rabbit antibody (1:200, Invitrogen), for one hour at room temperature and nuclei counterstained with DAPI. Collagen type I is indicated by red fluorescence and nuclei are indicated by blue fluorescence. Four images were acquired per hydrogel, and analyzed using NIH Image J for average total fluorescence (arbitrary units) normalized to the number of nuclei in each image to determine the fluorescence per nuclei per hydrogel. For the TUNEL and collagen I stains, sections were stained at the same time and imaged, under the same settings, using a laser scanning confocal microscope. Sections were stained for mineralization following standard protocols for von Kossa staining. Sections were treated with 1% (w/w) silver nitrate (Sigma) under ultraviolet light for 30 minutes. Unreacted silver was removed by 5% (w/w) sodium thiosulfate (Sigma) for 5 minutes at room temperature. Sections were counterstained with nuclear fast red (RICCA Chemical Company). Sections were imaged using light microscopy (Axiovert 40 C Zeiss). Mineralization stains black and nuclei stain pink to red.

2.9 DNA, Biochemical, and Cytokine Assays

Hydrogels (n = 3) were collected on days 0 (i.e., one day after encapsulation), 10, and 28, flash frozen with nuclease-free water in liquid nitrogen, and stored at -70^0C. Gels were homogenized for 5 minutes at 30 Hz using a Qiagen TissueLyser II. Homogenized samples were assessed for ALP activity using *p*-nitrophenol phosphate with *p*-nitrophenol used as a positive control and for Calcium content by using the Calcium (CPC) Liquicolor Assay kit

(Stanbio). DNA was quantified using the Quant-iT PicoGreen dsDNA assay kit (Invitrogen). Media from each sample were collected and flash frozen on day 10, which represents conditioned medium from day 8 to day 10, and on day 28, which represents conditioned medium from day 26 to day 28. Media samples were assessed for cytokines interleukin-6 (IL-6) and tumor necrosis factor alpha (TNF-α) using standard enzyme-linked immunosorbent assay kits (ELISA, R&D Systems for TNF-α, eBioscience for IL-6).

2.10 Statistical analysis

Data are presented as the mean of hydrogel replicates, sample size given above, with standard deviation as error bars in all plots and parenthetically in the text. Statistical analysis was performed using the XLSTAT add-in software for Microsoft Excel ® with a two-way unbalanced ANOVA (Table 1). Factors were culture time (day 0, 10, 28) and treatment type (± RAW264.7, ± primary macrophage, ±LPS). Comparisons were made using a Tukey post-hoc analysis with $\alpha = 0.05$. *P*-values of 0.1 or less are reported to indicate level of significance with a $p < 0.05$ considered to be statistically significant.

2.11 IACUC approval

All animal protocols were approved by the University of Colorado at Boulder Institutional Animal Care and Use Committee (IACUC) and follow the NIH guidelines for care and use of laboratory animals.

3. Results

An *in vitro* model system was designed to study the effects of macrophages on MC3T3-E1 cells encapsulated in a 3D bone mimetic PEG hydrogel containing MMP-sensitive crosslinks, the cell adhesion peptide, RGD, and hydroxyapatite nanoparticles (Fig. 1A). The cell-laden hydrogel was cultured under six experimental treatment conditions to simulate the FBR *in vitro*, which included mono-culture, co-culture with either RAW 264.7 macrophages or primary macrophages, and in each condition culture medium supplemented with or without LPS. Time, treatment, and their interaction were investigated as factors (Table 1). The experimental set-up is shown in Fig. 1B. Osteogenic medium was chosen for all cultures. RAW 264.7 macrophages and primary macrophages were refreshed weekly while LPS was refreshed every 48 hours.

3.1 Characterization of the acellular hydrogel

The hydrogel without cells was characterized with and without the incorporation of hydroxyapatite nanoparticles. The presence of hydroxyapatite nanoparticles was confirmed using Raman spectroscopy (Fig. 2A). The characteristic hydroxyapatite peak at 960 cm^{-1} was absent in hydrogels without hydroxyapatite nanoparticles and clearly present in the hydrogels with 1% hydroxyapatite nanoparticles. Hydroxyapatite appeared to be well dispersed within the hydrogel by brightfield microscopy (Supplemental information, Fig. S1). Further, the incorporation of hydroxyapatite nanoparticles did not significantly alter the compressive modulus (Fig. 2B) or volumetric equilibrium swelling ratio (Fig. 2C) of the hydrogels. The size of hydroxyapatite nanoparticles was determined from FESEM and the distribution of size is shown in Fig. 2D. A representative SEM image is provided in

supplemental information (Fig. S2). The average hydrogel mesh size of the hydrogel was determined to be 61.3(4.3) nm. The average size of the hydroxyapatite nanoparticles was determined to be 97.5(24.6) nm.

3.2 The effect of macrophages on MC3T3-E1 cell apoptosis and DNA content

The effect of LPS, macrophages, and their combination on MC3T3-E1 apoptosis in the 3D biomimetic hydrogel was assessed with culture time by TUNEL staining (Fig 3A,B). Though not a holistic characterization of cell viability, TUNEL stain allows for the visualization of cells that have undergone DNA degradation due to apoptosis. The percentage of apoptotic cells was affected by time ($p < 0.0001$) and treatment ($p = 0.019$) (Table 1). Initially, fewer than 1% of cells stained positive for apoptosis. Culture with RAW 264.7 macrophages did not lead to significant differences in the percentage of apoptotic cells. Culture with primary macrophages increased apoptosis by 6% at 10 days ($p = 0.04$) and 12% by 28 days ($p = 0.002$) from the initial time point. LPS stimulation did not significantly affect the percentage of apoptotic cells, whether alone or in co-culture with macrophages.

DNA content for the MC3T3-E1 cells in the hydrogels was assessed over time (Fig. 3C). After 28 days, mono-cultures and co-cultures with primary macrophages, independent of LPS activation, exhibited increases in DNA content. DNA content in co-cultures with RAW 264.7 macrophages was similar at the time points measured.

3.3 The effect of macrophages on MC3T3-E1 morphology

The morphology of the encapsulated MC3T3-E1 cells in the 3D biomimetic hydrogel was qualitatively assessed by confocal microscopy as a function of LPS, macrophages, and their combination (Fig. 4). Initially, the MC3T3-E1 cells displayed a round morphology. At 10 days of culture, the majority of the MC3T3-E1 cells within the hydrogels exhibited signs of cell spreading evident by extended cellular processes. With the addition of LPS, cell spreading was still evident. However, when cultured in the presence of RAW 264.7 macrophages with or without LPS, MC3T3-E1 cells retained their rounded morphology with no observable signs of cell spreading. In the presence of primary macrophages, there were evidence of cell spreading, as well as rounded cells. When cultured with LPS and in the presence of primary macrophages, MC3T3-E1 cell spreading appeared to be reduced, but not inhibited. These results indicate that while MC3T3-E1 cells are capable of spreading within the biomimetic hydrogel, the presence of RAW 264.7 macrophages and to a lesser extent primary macrophages inhibit MC3T3-E1 cell spreading. LPS stimulation appeared to have minimal effects.

3.4 The effects of macrophages on collagen I deposition by MC3T3-E1 cells

MC3T3-E1 cell-laden biomimetic hydrogels were assessed for collagen I deposition initially and after 10 and 28 days in culture as a function of LPS, macrophages, and their combination (Fig. 5). Representative confocal microscopy images are shown in Fig. 5A along with quantitative analysis in Fig. 5B. Initially, the MC3T3-E1 cells stained for collagen I, but the staining was largely localized in what appeared to be the intracellular regions. At day 10, MC3T3-E1 cells deposited collagen I that formed an interconnected

matrix within aggregates of cells. Similar results were observed at day 28. With the addition of LPS, aggregates of cells with an interconnected matrix of collagen I were evident, but the staining was not as pronounced. In the presence of RAW 264.7 macrophages, collagen I staining was evident, but it was localized the pericellular region at day 10 and remained localized at day 28. Treatment with LPS did not appear to affect the spatial organization of collagen I. Similar results were observed with primary macrophages. Fluorescence intensity of the collagen I stain per nuclei was quantified as a measure of collagen I content. Collagen I was affected by time ($p < 0.0001$) and treatment ($p < 0.0001$) (Table 1). In mono-culture without LPS stimulation, collagen I increased ($p = 0.0004$) from day 0 to day 10 and then remained constant at day 28. With LPS stimulation, collagen I increased but not to the same extent at day 10, but by day 28 was similar regardless of LPS. In co-culture with RAW 264.7 macrophages regardless of LPS stimulation, collagen I was lower ($p < 0.0001$ without LPS and $p = 0.0004$ with LPS) at day 28 when compared to the unstimulated mono-cultures. In co-culture with primary macrophages, collagen I increased ($p = 0.003$) by day 28 without LPS, but was slightly lower ($p = 0.053$) than unstimulated mono-cultures. However, with LPS, collagen I was not different from day 0 and lower ($p <0.001$) when compared to unstimulated mono-cultures. Large standard deviations at later time points (day 28) are attributed to heterogeneities that form as the hydrogel degrades and neotissue is deposited, which have been reported previously [39]. Overall, the presence of RAW 264.7 or primary macrophages with LPS inhibited collagen I deposition by the MC3T3-E1 cells at 28 day.

3.5 The effects of macrophages on ALP activity and mineralization in MC3T3-E1-laden biomimetic hydrogels

MC3T3-E1 cell-laden biomimetic hydrogels were assessed for alkaline phosphatase (ALP) activity (Fig. 6A), total calcium content (Fig. 6B), and spatial organization of mineral deposition (Fig. 6C) as a function of LPS, macrophages, and their combination. ALP activity was affected by time ($p = 0.012$) and treatment ($p < 0.0001$) (Table 1). At day 10, the unstimulated mono-cultures of the MC3T3-E1 cells in the hydrogels had the highest ($p < 0.0001$) ALP activity compared to all other treatments at the same timepoint, and was approximately threefold higher ($p < 0.0001$) when compared to the initial time point. For all other treatment conditions at day 10, ALP activity was not different to the initial time point. At day 28, ALP activity in the mono-cultures returned to initial levels. In the co-culture with RAW 264.7 macrophages at day 28, stimulated with LPS or not, MC3T3-E1 cells had the higher ($p < 0.0001$) ALP activity when compared to the mono-culture of the MC3T3-E1 cell-laden hydrogels without LPS. However, in co-culture with primary macrophages, stimulated with LPS or not, ALP activity was similar to initial levels.

Mineralization was assessed by total calcium and von Kossa staining. Total calcium content per hydrogel was affected by time ($p < 0.0001$), but not by treatment (Table 1). The initial time point represents calcium that is from the entrapped hydroxyapatite nanoparticles and any residual calcium from the culture medium. Any increase in calcium content is attributed to mineral deposition that occurred during culture. Total calcium content increased ($p < 0.0001$) from day 0 to day 10. There was no significant change in total calcium content from day 10 to day 28. Spatial organization of mineral deposition was qualitatively assessed through von Kossa staining. At day 0, minimal mineral deposition was detected.

Qualitatively, mineral deposition was apparent by day 10 and present in all treatment conditions. At day 10, MC3T3-E1 cell-laden hydrogels cultured with RAW 264.7 macrophages, regardless of LPS, appeared to show more elaborate mineral deposition throughout the construct when compared to the mono-culture and the co-culture with primary macrophages. At day 28, mineral deposition was pronounced throughout all of the hydrogels with no observable differences among treatment conditions.

3.6 Cytokine secretion from the in vitro co-culture model

To characterize the inflammatory environment in the co-culture model, secretion of interleukin-6 (IL-6) (Fig. 7A) and tumor necrosis factor-alpha (TNF-α) (Fig. 7B) into the culture medium was quantified by ELISA at select time points of day 10 and day 28, which corresponded to all of the other assessments of the hydrogel. The media at day 10 represents conditioned media from day 8–10, and the media at day 28 represents conditioned media from day 26–28. Monitoring of the temporal changes in cytokine secretion beyond these discrete time points was not assessed. IL-6 was not affected by time or treatment independently, but there was a crossover interaction (Table 1). At day 10 in the absence of LPS stimulation, IL-6 levels were undetectable in the mono-culture and co-culture with RAW 264.7 and primary macrophages. At day 10 with LPS stimulation, there was pronounced IL-6 levels in the mono-culture and co-culture with RAW 264.7 and primary macrophages. At day 28, IL-6 levels were detectable in the mono-culture and in the co-culture with primary macrophages without LPS. With LPS, IL-6 levels were detectable, but lower ($p = 0.01$ for mono-culture; $p < 0.001$ for co-culture) when compared to their respective treatment without LPS. The co-culture with RAW 264.7 macrophages did not have detectable levels of IL-6 at day 28.

TNF- α was affected by time ($p = 0.023$) and treatment ($p < 0.0001$) and there was a significant interaction between time and treatment (Table 1). Secretion of TNF-α was not detected in the mono-culture without LPS at day 10 nor at day 28, but was detectable at day 28 with LPS. In the co-culture with RAW 264.7 macrophages, TNF-α levels were ~60 pg/ml and increased ($p = 0.002$) by 10-fold with LPS at day 10. At day 28, TNF-α was not detectable in the co-culture with RAW 264.7 macrophages without LPS, but was detectable with LPS stimulation. In the co-culture with primary macrophages, TNF-α was not detectable in the culture without LPS at day 10, but was detected at ~40 pg/ml with LPS at day 10. At day 28, TNF-α levels in co-culture with primary macrophages were detected at ~46 pg/mL without LPS and were higher ($p = 0.03$) with LPS.

4. Discussion

Though PEG hydrogels are promising cell delivery vehicles for tissue engineering [40], their induction of a FBR *in vivo* raises questions for *in vivo* tissue engineering. This study identified that macrophages elevated MC3T3-E1 cell apoptosis, reduced cell spreading, delayed or inhibited alkaline phosphatase activity, and decreased collagen elaboration, but did not affect mineralization. Although both macrophages sources had a negative effect on the MC3T3-E1 cells, primary macrophages were more potent. Collectively, this study demonstrates that while MC3T3-E1 cells are capable of differentiating and depositing bone-

like ECM in the presence of macrophages and the inflammatory stimulant LPS, this process is significantly impaired.

The biomimetic hydrogel with hydroxyapatite nanoparticles supported MC3T3-E1 differentiation and deposition of bone ECM in the absence of macrophages and LPS. MC3T3-E1 cell spreading was evident within the hydrogel, which is attributed to the combined presence of RGD and MMP-sensitive crosslinks [21]. Osteogenic differentiation was confirmed by increased ALP activity, a known early marker of osteogenesis. Bone ECM deposition was evident by collagen I and mineralized matrix present throughout the hydrogel construct. The cells also secreted IL-6, but no measurable TNF-α. IL-6 has been linked to osteoblast differentiation and maturation [43,44]. Overall, these results confirm that the bone-mimetic hydrogel is promising for bone tissue engineering and thus is a suitable system to assess the effects of a simulated FBR on the encapsulated cells and their ability to synthesize ECM.

Chronic inflammation, which is a part of the FBR, is known to induce programmed cell death and contribute to tissue injury [45]. Overall the percentage apoptotic MC3T3-E1 cells remained below ~15% during the 28 day culture regardless of condition. Primary macrophages had the most significant effect on MC3T3-E1 apoptosis over the untreated hydrogels. LPS did not have any additional effect, suggesting that macrophages on their own are capable of inducing apoptosis. Long-term exposure of the MC3T3-E1 cells to LPS alone did not induce apoptosis, which is contrary to other studies [46,47]. This difference is attributed to the 3D culture, where these previous studies were done in 2D cultures. These findings demonstrate that macrophages in the absence of LPS stimulation are able to induce MC3T3-E1 apoptosis, albeit at low levels, in the *in vitro* co-culture model.

The biomimetic hydrogel created an environment whereby encapsulated MC3T3-E1 cells locally degraded the hydrogel enabling extension of their cellular processes and cell spreading. The presence of macrophages reduced or inhibited MC3T3-E1 cell spreading, which was most pronounced in the presence of RAW 264.7 macrophages. Studies with osteogenically differentiating MC3T3-E1 cells have reported increased expression MMP-2 [48]. Thus, it is possible that an inhibition in osteogenesis, due to the simulated FBR environment with macrophages, led to the reduction in MMP activity and a subsequent reduction in cell spreading, which may further slow differentiation [49,50]. We have previously reported that macrophages *in vitro* do not rapidly degrade this MMP-sensitive crosslinker in a PEG hydrogel, whether by direct culture or through conditioned medium, nor does the hydrogel undergo rapid degradation *in vivo* [21]. Additional studies are needed to identify the exact mechanism(s) that contributed to the observed reduction of cell spreading.

Osteogenic differentiation of the MC3T3-E1 cells, as measured by ALP activity, was affected by LPS, macrophages and their combination. An inflammatory environment has been shown to be detrimental to osteogenesis [51]. At 10 days, ALP activity was inhibited under all inflammatory conditions. LPS and pro-inflammatory cytokines (e.g., TNF- α) act by up-regulating NF-κB signaling [52], which has been shown to inhibit ALP activity in osteoblast-like cells [53]. Interestingly, an increase in ALP activity was observed by day 28

in MC3T3-E1 cells, but only in those cultured with RAW 264.7 macrophages. Because ALP activity generally peaks between ~7–14 days in culture [54], this result suggests a delay in osteogenic differentiation. This finding was not observed with the primary macrophages, but it is possible that a peak in ALP activity was not captured due to the selected time points. Nonetheless, these data indicate that the inflammatory environment, resulting from LPS and/or macrophages, delays or inhibits osteogenic differentiation in the bone-mimetic hydrogels.

The *in vitro* simulated FBR differentially affected ECM deposition by the MC3T3-E1 cells in the bone-mimetic hydrogel. At day 10, collagen deposition was present under all inflammatory conditions, but substantially reduced when compared to the untreated condition. Collagen synthesis has been shown to be highly susceptible to the presence of pro-inflammatory cytokines [55]. In this study, macrophages had the most significant negative effect on collagen I deposition, indicating that their secreted factors are more potent over LPS alone. The observed reduction in collagen I deposition is attributed to an inhibition in collagen synthesis. Since the hydrogel, which is susceptible to similar MMPs as collagen, did not undergo rapid degradation, it is unlikely that the reduced collagen was due to its degradation. Moreover, the reduced cell spreading and ALP activity point to a delay in osteogenesis, which would also explain the delay in collagen synthesis.

On the other hand, mineralization in the bone-mimetic hydrogels was not sensitive to the *in vitro* simulated FBR. Mineralization requires mineral precursors and nucleation sites [56], which can be found in matrix vesicles [42]. Upon their breakdown, these mineral precursors are then exposed to ECM (e.g., collagen), where mineralization is regulated [57]. By incorporating hydroxyapatite particles directly into the bone-mimetic hydrogel, it is possible to “bypass” the phosphatase-controlled vesicle phase of mineralization. Alternatively, it has been reported that pro-inflammatory cytokines induce a mineralizing phenotype in bone marrow-derived mesenchymal stem cells [58]. This mineralization pathway still necessitates ALP activity, but the threshold is much lower for mineralization to occur [58]. While we reported high levels of ALP only in the untreated hydrogels cultures, it is possible that since the MC3T3-E1 cells are initially pre-osteoblasts, they may display basal levels of ALP activity that are above the threshold to induce inflammation-mediated mineralization. Thus, mineralization may occur even if differentiation is inhibited. The presence of mineral, which is known to be osteoinductive, may help to overcome the initial negative effects of the inflammatory environment and thus could explain the observed delay in differentiation.

Towards characterizing the inflammatory environment in the co-culture system, pro-inflammatory cytokines IL-6 and TNF-α were investigated. Pro-inflammatory cytokine secretion is known to direct cross talk and differentiation between macrophages and other cells [59,60]. IL-6 is a multifunctional cytokine that regulates a diverse range of functions from inflammation to homeostasis [61]. In bone, the role of IL-6 is primarily understood as a promotor of osteoclastogenesis and important to bone regeneration, but studies on its role in osteoblast differentiation have been conflicting [62–64]. The role of TNF-α in bone homeostasis is more well-defined, where studies have reported inhibition of osteoblast differentiation and activity by TNF-α [64]. LPS stimulation leads to NF-κB induced expression of IL-6 and TNF-α, which has been shown in macrophages and mature

osteoblasts [52,68,69]. At day 10, IL-6 was only detectable in the LPS stimulated conditions, which points to LPS-mediated induction of IL-6 by both MC3T3-E1 cells and macrophages. Interestingly, only co-culture with primary macrophages and LPS led to detectable amounts of both cytokines at the two time points investigated. This condition correlated with significant apoptosis, inhibition in ALP activity, and reduction in collagen deposition. Taken together, these findings confirm that with LPS and/or macrophages, TNF-α is secreted at some point during the culture period and thus may contribute to the adverse effects in the MC3T3-E1 cells in the bone mimetic hydrogel.

We investigated two murine macrophage sources, the commonly used cell line, RAW 264.7, and bone marrow-derived macrophages. Several studies have reported that macrophage phenotype differs depending on the cell source [34,70], despite their often interchangeable use in *in vitro* studies. Importantly, our results indicate that both macrophage sources have a negative impact on the MC3T3-E1 cells in the bone-mimetic hydrogel. However, primary macrophages stimulated with LPS appeared to have the greatest adverse effect on the MC3T3-E1 cells leading to significantly higher apoptosis, reduced collagen I deposition, low ALP activity, and had measurable levels of both IL-6 and TNF-α at the time points investigated. This result is consistent with other studies which have shown that macrophage cell lines have been noted to exhibit lower pro-inflammatory cytokine secretion than primary macrophages [35,36]. Either RAW264.7 or primary macrophages can serve as a useful macrophage source in this *in vitro* model. However, findings from this study suggest primary macrophages are a better choice for simulating the FBR *in vitro* given that they are more potent and provide a more “direct” comparison to the *in vivo* environment.

There are several limitations of this work. This study focused on the effects that macrophages have on MC3T3-E1 cells in a biomimetic PEG hydrogel system. However, we have previously shown that crosstalk between encapsulated cells and macrophages can influence macrophage activation [24]. Thus, it is possible that the crosstalk between MC3T3-E1 cells and osteoblasts may have activated macrophages in the absence of LPS. Future studies will need to assess the effect that MC3T3-E1 cells have on macrophage activation to understand the full extent of the crosstalk. Additionally, the scope of this study focused on paracrine signaling between macrophages and the encapsulated cells. The synergistic effect of the biomaterial and juxtacrine signaling will need to be investigated in the future. A culture medium optimized for the MC3T3-E1 cells was chosen to assess their differentiation and ECM synthesis. Because macrophages are migratory and found in all tissues in the body, we expect that the readily adapt to different environments; however, the media was not optimized for macrophages. Another limitation was that the assessment of the cytokines levels was limited to two discrete time points that corresponded to the assessment of differentiation and ECM deposition. Further experiments are required to characterize the full spectrum of paracrine factors and identify the factors that led to the adverse effects on the pre-osteoblast cells. Finally, culture times beyond four weeks will be needed to determine the long-term impact of macrophages and an inflammatory environment on tissue growth both *in vitro* and *in vivo*.

5. Conclusions

Our *in vitro* studies show that inflammatory macrophages can impact osteoblastic cells, leading to decreased cell spreading within MMP-sensitive PEG hydrogels, reduced alkaline phosphatase activity, and lower collagen I deposition. Importantly, our findings implicate that the FBR, as shown here through *in vitro* simulated conditions, can delay osteogenesis and slow bone ECM deposition. Future work will need to determine how the *in vivo* scenario and the FBR, which is more complex than the *in vitro* experiments, affects tissue growth. Further, given that many cell types are sensitive to an inflammatory environment [71,72], macrophages may have a detrimental effect on other cell types and biomaterials for tissue regeneration and warrant further study. In summary, the FBR to non-biological scaffolds may have a negative effect on the ability of the embedded cells to synthesize and deposit new tissue. Thus, biomaterial designs that reduce the FBR may be critical to improving tissue regeneration capabilities of encapsulated cells.

Supplementary Material

Refer to Web version on PubMed Central for supplementary material.

6. Acknowledgments

This research was supported by the National Institute of Arthritis and Musculoskeletal and Skin Diseases of the National Institutes of Health under Award Number R21AR064436 and 1R01AR069060. The content is solely the responsibility of the authors and does not necessarily represent the official views of the National Institutes of Health. The authors also acknowledge support from a Department of Education GAANN fellowship to LSS, and the Balsells Fellowship to MCC.

References

[1]. McCall JD, Luoma JE, Anseth KS, Covalently tethered transforming growth factor beta in PEG hydrogels promotes chondrogenic differentiation of encapsulated human mesenchymal stem cells, Drug Deliv. Transl. Res. 2 (2012) 305–312. doi:10.1007/s13346-012-0090-2. [PubMed: 23019539]

[2]. Raza A, Lin CC, The influence of matrix degradation and functionality on cell survival and morphogenesis in PEG-based hydrogels, Macromol. Biosci. 13 (2013) 1048–1058. doi:10.1002/mabi.201300044. [PubMed: 23776086]

[3]. Sokic S, Papavasiliou G, Controlled proteolytic cleavage site presentation in biomimetic PEGDA hydrogels enhances neovascularization in vitro., Tissue Eng. Part A. 18 (2012) 2477–86. doi:10.1089/ten.TEA.2012.0173. [PubMed: 22725267]

[4]. Adelöw C, Segura T, Hubbell J. a., Frey P, The effect of enzymatically degradable poly(ethylene glycol) hydrogels on smooth muscle cell phenotype, Biomaterials. 29 (2008) 314–326. doi:10.1016/j.biomaterials.2007.09.036. [PubMed: 17953986]

[5]. Amer LD, Holtzinger A, Keller G, Mahoney MJ, Bryant SJ, Enzymatically degradable poly(ethylene glycol) hydrogels for the 3D culture and release of human embryonic stem cell derived pancreatic precursor cell aggregates, Acta Biomater. 22 (2015) 103–110. doi:10.1016/j.actbio.2015.04.013. [PubMed: 25913222]

[6]. Van Hove AH, Burke K, Antonienko E, Brown E, Benoit DSW, Enzymatically-responsive pro-angiogenic peptide-releasing poly(ethylene glycol) hydrogels promote vascularization in vivo, J. Controlled Release. 217 (2015) 191–201. doi:10.1016/j.jconrel.2015.09.005.

[7]. Mesure L, Visscher GD, Vranken I, Lebacq A, Flameng W, Gene Expression Study of Monocytes/Macrophages during Early Foreign Body Reaction and Identification of Potential Precursors of Myofibroblasts, PLOS ONE. 5 (2010) e12949. doi:10.1371/journal.pone.0012949.

[8]. Anderson JM, Rodriguez A, Chang DT, Foreign body reaction to biomaterials., Semin. Immunol. 20 (2008) 86–100. doi:10.1016/j.smim.2007.11.004. [PubMed: 18162407]

[9]. Bryant SJ, Ratner BD, Biomaterials: Where We Have Been and Where We Are Going, Annu. Rev. Biomed. Eng. 6 (2004) 41–75. doi:10.1146/annurev.bioeng.6.040803.140027. [PubMed: 15255762]

[10]. Zhang L, Cao Z, Bai T, Carr L, Ella-Menye J-R, Irvin C, Ratner BD, Jiang S, Zwitterionic hydrogels implanted in mice resist the foreign-body reaction., Nat. Biotechnol. 31 (2013) 553–6. doi:10.1038/nbt.2580. [PubMed: 23666011]

[11]. Delgado LM, Bayon Y, Pandit A, Zeugolis DI, To Cross-Link or Not to Cross-Link? Cross-Linking Associated Foreign Body Response of Collagen-Based Devices, Tissue Eng. Part B Rev. 21 (2015) 298–313. doi:10.1089/ten.teb.2014.0290. [PubMed: 25517923]

[12]. Cadée J. a., van Luyn M. j. a., Brouwer L. a., Plantinga J. a., van Wachem P. b., de Groot C. j., den Otter W, Hennink W. e., In vivo biocompatibility of dextran-based hydrogels, J. Biomed. Mater. Res. 50 (2000) 397–404. doi:10.1002/(SICI)1097-4636(20000605)50:3<397::AID-JBM14>3.0.CO;2-A. [PubMed: 10737882]

[13]. Veiseh O, Doloff JC, Ma M, Vegas AJ, Tam HH, Bader AR, Li J, Langan E, Wyckoff J, Loo WS, Jhunjhunwala S, Chiu A, Siebert S, Tang K, Hollister-Lock J, Aresta-Dasilva S, Bochenek M, Mendoza-Elias J, Wang Y, Qi M, Lavin DM, Chen M, Dholakia N, Thakrar R, Lacík I, Weir GC, Oberholzer J, Greiner DL, Langer R, Anderson DG, Size- and shape-dependent foreign body immune response to materials implanted in rodents and non-human primates, Nat. Mater. 14 (2015) 643–651. doi:10.1038/nmat4290. [PubMed: 25985456]

[14]. Swartzlander MD, Bryant SJ, Linking the foreign body response and protein adsorption to PEG-based hydrogels using proteomics, Biomaterials. 41 (2015) 26–36. doi:10.1016/j.biomaterials.2014.11.026. [PubMed: 25522962]

[15]. Kim J, Dadsedan M, Ameenuddin S, Windebank AJ, Yaszemski MJ, Lu L, In Vivo Biodegradation and Biocompatibility of PEG/Sebacic Acid-Based Hydrogels using a Cage Implant System, J. Biomed. Mater. Res. A. 95 (2010) 191–197. doi:10.1002/jbm.a.32810. [PubMed: 20574982]

[16]. Burdick JA, Padera RF, Huang JV, Anseth KS, An investigation of the cytotoxicity and histocompatibility of in situ forming lactic acid based orthopedic biomaterials, J. Biomed. Mater. Res. 63 (2002) 484–491. doi:10.1002/jbm.10298. [PubMed: 12209891]

[17]. Suggs LJ, Mikos AG, Development of poly(propylene fumarate-co-ethylene glycol) as an injectable carrier for endothelial cells, Cell Transplant. 8 (1999) 345–350. [PubMed: 10478714]

[18]. Riedel T, Riedelová-Reicheltová Z, Májek P, Rodriguez-Emmenegger C, Houska M, Dyr JE, Brynda E, Complete Identification of Proteins Responsible for Human Blood Plasma Fouling on Poly(ethylene glycol)-Based Surfaces, Langmuir. 29 (2013) 3388–3397. doi:10.1021/la304886r. [PubMed: 23391268]

[19]. Huang W-C, Sala-Newby GB, Susana A, Johnson JL, Newby AC, Classical macrophage activation up-regulates several matrix metalloproteinases through mitogen activated protein kinases and nuclear factor-κB., PloS One. 7 (2012) e42507. doi:10.1371/journal.pone.0042507.

[20]. Brodbeck WG, Nakayama Y, Matsuda T, Colton E, Ziats NP, Anderson JM, Biomaterial surface chemistry dictates adherent monocyte/macrophage cytokine expression in vitro., Cytokine. 18 (2002) 311–319. doi:10.1006/cyto.2002.1048. [PubMed: 12160519]

[21]. Amer LD, Bryant SJ, The In Vitro and In Vivo Response to MMP-Sensitive Poly(Ethylene Glycol) Hydrogels, Ann. Biomed. Eng. 44 (2016) 1959–1969. doi:10.1007/s10439-016-1608-4. [PubMed: 27080375]

[22]. Swartzlander MD, Blakney AK, Amer LD, Hankenson KD, Kyriakides TR, Bryant SJ, Immunomodulation by mesenchymal stem cells combats the foreign body response to cell-laden synthetic hydrogels, Biomaterials. 41 (2015) 79–88. doi:10.1016/j.biomaterials.2014.11.020. [PubMed: 25522967]

[23]. Lynn AD, Blakney AK, Kyriakides TR, Bryant SJ, Temporal progression of the host response to implanted poly(ethylene glycol)-based hydrogels., J. Biomed. Mater. Res. A. 96 (2011) 621–31. doi:10.1002/jbm.a.33015. [PubMed: 21268236]

[24]. Swartzlander MD, Lynn AD, Blakney AK, Kyriakides TR, Bryant SJ, Understanding the host response to cell-laden poly(ethylene glycol)-based hydrogels., Biomaterials. 34 (2013) 952–64. doi:10.1016/j.biomaterials.2012.10.037. [PubMed: 23149012]

[25]. Asawa Y, Sakamoto T, Komura M, Watanabe M, Nishizawa S, Takazawa Y, Takato T, Hoshi K, Early stage foreign body reaction against biodegradable polymer scaffolds affects tissue regeneration during the autologous transplantation of tissue-engineered cartilage in the canine model, Cell Transplant. 21 (2012) 1431–1442. doi:10.3727/096368912X640574. [PubMed: 22546666]

[26]. Shin H, Quinten Ruhé P, Mikos AG, Jansen JA, In vivo bone and soft tissue response to injectable, biodegradable oligo(poly(ethylene glycol) fumarate) hydrogels, Biomaterials. 24 (2003) 3201–3211. doi:10.1016/S0142-9612(03)00168-6. [PubMed: 12763447]

[27]. Lin C-C, Raza A, Shih H, PEG hydrogels formed by thiol-ene photo-click chemistry and their effect on the formation and recovery of insulin-secreting cell spheroids., Biomaterials. 32 (2011) 9685–95. doi:10.1016/j.biomaterials.2011.08.083. [PubMed: 21924490]

[28]. Mariner PD, Wudel JM, Miller DE, Genova EE, Streubel SO, Anseth KS, Synthetic hydrogel scaffold is an effective vehicle for delivery of INFUSE (rhBMP2) to critical-sized calvaria bone defects in rats, J. Orthop. Res. 31 (2013) 401–406. doi:10.1002/jor.22243. [PubMed: 23070779]

[29]. Fairbanks BD, Schwartz MP, Halevi AE, Nuttelman CR, Bowman CN, Anseth KS, A Versatile Synthetic Extracellular Matrix Mimic via Thiol-Norbornene Photopolymerization, Adv. Mater. 21 (2009) 5005–5010. doi:10.1002/adma.200901808. [PubMed: 25377720]

[30]. Lin C-C, Ki CS, Shih H, Thiol-norbornene photoclick hydrogels for tissue engineering applications, J. Appl. Polym. Sci. 132 (2015). doi:10.1002/app.41563.

[31]. Roberts JJ, Bryant SJ, Comparison of photopolymerizable thiol-ene PEG and acrylate-based PEG hydrogels for cartilage development., Biomaterials. 34 (2013) 9969–79. doi:10.1016/j.biomaterials.2013.09.020. [PubMed: 24060418]

[32]. Xu K, Fu Y, Chung W, Zheng X, Cui Y, Hsu IC, Kao WJ, Thiol–ene-based biological/synthetic hybrid biomatrix for 3-D living cell culture, Acta Biomater. 8 (2012) 2504–2516. doi:10.1016/j.actbio.2012.03.049. [PubMed: 22484717]

[33]. Jay SM, Skokos E, Laiwalla F, Krady M-M, Kyriakides TR, Foreign body giant cell formation is preceded by lamellipodia formation and can be attenuated by inhibition of Rac1 activation., Am. J. Pathol. 171 (2007) 632–640. doi:10.2353/ajpath.2007.061213. [PubMed: 17556592]

[34]. Chamberlain LM, Godek ML, Gonzalez-Juarrero M, Grainger DW, Phenotypic non-equivalence of murine (monocyte-) macrophage cells in biomaterial and inflammatory models., J. Biomed. Mater. Res. A. 88 (2009) 858–71. doi:10.1002/jbm.a.31930. [PubMed: 18357567]

[35]. Heil TL, Volkmann KR, Wataha JC, Lockwood PE, Human peripheral blood monocytes versus THP-1 monocytes for in vitro biocompatibility testing of dental material components, J. Oral Rehabil. 29 (2002) 401–407. doi:10.1046/j.1365-2842.2002.00893.x. [PubMed: 12028485]

[36]. Pan C, Kumar C, Bohl S, Klingmueller U, Mann M, Comparative Proteomic Phenotyping of Cell Lines and Primary Cells to Assess Preservation of Cell Type-specific Functions, Mol. Cell. Proteomics. 8 (2009) 443–450. doi:10.1074/mcp.M800258-MCP200. [PubMed: 18952599]

[37]. Canal T, Peppas NA, Correlation between mesh size and equilibrium degree of swelling of polymeric networks, J. Biomed. Mater. Res. 23 (1989) 1183–1193. doi:10.1002/jbm.820231007. [PubMed: 2808463]

[38]. Akalp U, Chu S, Skaalure SC, Bryant SJ, Doostan A, Vernerey FJ, Determination of the Polymer-Solvent Interaction Parameter for PEG Hydrogels in Water: Application of a Self Learning Algorithm, Polymer. 66 (2015) 135–147. doi:10.1016/j.polymer.2015.04.030. [PubMed: 25999615]

[39]. Schneider MC, Chu S, Sridhar SL, de Roucy G, Vernerey FJ, Bryant SJ, Local Heterogeneities Improve Matrix Connectivity in Degradable and Photoclickable Poly(ethylene glycol) Hydrogels for Applications in Tissue Engineering, ACS Biomater. Sci. Eng. 3 (2017) 2480–2492. doi:10.1021/acsbiomaterials.7b00348. [PubMed: 29732400]

[40]. Lowe S, O'Brien-Simpson NM, Connal L. a., Antibiofouling polymer interfaces: poly(ethylene glycol) and other promising candidates, Polym Chem. 6 (2015) 198–212. doi:10.1039/C4PY01356E.

[41]. Taguchi Y, Yamamoto M, Yamate T, Lin SC, Mocharla H, DeTogni P, Nakayama N, Boyce BF, Abe E, Manolagas SC, Interleukin-6-type cytokines stimulate mesenchymal progenitor differentiation toward the osteoblastic lineage., Proc. Assoc. Am. Physicians. 110 (1998) 559–574. [PubMed: 9824538]

[42]. Li Y, Bäckesjö C-M, Haldosén L-A, Lindgren U, IL-6 receptor expression and IL-6 effects change during osteoblast differentiation, Cytokine. 43 (2008) 165–173. doi:10.1016/j.cyto.2008.05.007. [PubMed: 18555695]

[43]. Wallach D, Kang T-B, Kovalenko A, Concepts of tissue injury and cell death in inflammation: a historical perspective, Nat. Rev. Immunol. 14 (2014) 51–59. doi:10.1038/nri3561. [PubMed: 24336099]

[44]. Guo C, Yuan L, Wang J, Wang F, Yang X-K, Zhang F, Song J, Ma X, Cheng Q, Song G, Lipopolysaccharide (LPS) Induces the Apoptosis and Inhibits Osteoblast Differentiation Through JNK Pathway in MC3T3-E1 Cells, Inflammation. 37 (2014) 621–631. doi:10.1007/s10753-013-9778-9. [PubMed: 24272171]

[45]. Raza H, John A, Shafarin J, Potentiation of LPS-Induced Apoptotic Cell Death in Human Hepatoma HepG2 Cells by Aspirin via ROS and Mitochondrial Dysfunction: Protection by N-Acetyl Cysteine, PLoS ONE. 11 (2016). doi:10.1371/journal.pone.0159750.

[46]. Hakki SS, Bozkurt SB, Hakki EE, Korkusuz P, Purali N, Koç N, Muharrem Timucin A Ozturk, Korkusuz F, Osteogenic differentiation of MC3T3-E1 cells on different titanium surfaces, Biomed. Mater. 7 (2012) 045006. doi:10.1088/1748-6041/7/4/045006.

[47]. Khetan S, Guvendiren M, Legant WR, Cohen DM, Chen CS, a Burdick J, Degradation-mediated cellular traction directs stem cell fate in covalently crosslinked three-dimensional hydrogels., Nat. Mater. 12 (2013) 458–65. doi:10.1038/nmat3586. [PubMed: 23524375]

[48]. Yang F, Williams CG, Wang D-A, Lee H, Manson PN, Elisseeff J, The effect of incorporating RGD adhesive peptide in polyethylene glycol diacrylate hydrogel on osteogenesis of bone marrow stromal cells., Biomaterials. 26 (2005) 5991–8. doi:10.1016/j.biomaterials.2005.03.018. [PubMed: 15878198]

[49]. Osta B, Benedetti G, Miossec P, Classical and paradoxical effects of TNF-a on bone homeostasis, Front. Immunol. 5 (2014) 1–9. doi:10.3389/fimmu.2014.00048. [PubMed: 24474949]

[50]. Schütze S, Wiegmann K, Machleidt T, Krönke M, TNF-induced activation of NF-kappa B, Immunobiology. 193 (1995) 193–203. [PubMed: 8530143]

[51]. Chang J, Wang Z, Tang E, Fan Z, McCauley L, Franceschi R, Guan K, Krebsbach PH, Wang C-Y, Inhibition of osteoblastic bone formation by nuclear factor-kappaB, Nat. Med. 15 (2009) 682–689. doi:10.1038/nm.1954. [PubMed: 19448637]

[52]. Beck GR, Sullivan EC, Moran E, Zerler B, Relationship between alkaline phosphatase levels, osteopontin expression, and mineralization in differentiating MC3T3-E1 osteoblasts, J. Cell. Biochem. 68 (1998) 269–280. doi:10.1002/(SICI)1097-4644(19980201)68:2<269::AID-JCB13>3.0.CO;2-A. [PubMed: 9443082]

[53]. Solis-Herruzo JA, Brenner DA, Chojkier M, Tumor necrosis factor alpha inhibits collagen gene transcription and collagen synthesis in cultured human fibroblasts., J. Biol. Chem. 263 (1988) 5841–5845. [PubMed: 3258601]

[54]. Weiner S, Organization of extracellularly mineralized tissues: a comparative study of biological crystal growth, CRC Crit. Rev. Biochem. 20 (1986) 365–408. [PubMed: 3524990]

[55]. Dean DD, Schwartz Z, Bonewald L, Muniz OE, Morales S, Gomez R, Brooks BP, Qiao M, Howell DS, Boyan BD, Matrix vesicles produced by osteoblast-like cells in culture become significantly enriched in proteoglycan-degrading metalloproteinases after addition of beta-glycerophosphate and ascorbic acid, Calcif. Tissue Int. 54 (1994) 399–408. [PubMed: 8062158]

[56]. Hunter GK, Hauschka PV, Poole a R., Rosenberg LC, Goldberg H. a, Nucleation and inhibition of hydroxyapatite formation by mineralized tissue proteins., Biochem. J. 317 (Pt 1 (1996) 59–64. [PubMed: 8694787]

[57]. Ferreira E, Porter RM, Wehling N, O'Sullivan RP, Liu F, Boskey A, Estok DM, Harris MB, Vrahas MS, Evans CH, Wells JW, Inflammatory Cytokines Induce a Unique Mineralizing Phenotype in Mesenchymal Stem Cells Derived from Human Bone Marrow, J. Biol. Chem. 288 (2013) 29494–29505. doi:10.1074/jbc.M113.471268. [PubMed: 23970554]

[58]. Souza PPC, Lerner UH, The role of cytokines in inflammatory bone loss., Immunol. Invest. 42 (2013) 555–622. doi:10.3109/08820139.2013.822766. [PubMed: 24004059]

[59]. Deshpande S, James AW, Blough J, Donneys A, Wang SC, Cederna PS, Buchman SR, Levi B, Reconciling the effects of inflammatory cytokines on mesenchymal cell osteogenic differentiation., J. Surg. Res. 185 (2013) 278–85. doi:10.1016/j.jss.2013.06.063. [PubMed: 23972621]

[60]. Gabay C, Interleukin-6 and chronic inflammation, Arthritis Res. Ther. 8 (2006) S3. doi:10.1186/ar1917.

[61]. Peruzzi B, Cappariello A, Fattore AD, Rucci N, Benedetti FD, Teti A, c-Src and IL-6 inhibit osteoblast differentiation and integrate IGFBP5 signalling, Nat. Commun. 3 (2012) ncomms1651. doi:10.1038/ncomms1651.

[62]. Franchimont N, Wertz S, Malaise M, Interleukin-6: An osteotropic factor influencing bone formation?, Bone. 37 (2005) 601–606. doi:10.1016/j.bone.2005.06.002. [PubMed: 16112634]

[63]. Itoh S, Udagawa N, Takahashi N, Yoshitake F, Narita H, Ebisu S, Ishihara K, A critical role for interleukin-6 family-mediated Stat3 activation in osteoblast differentiation and bone formation, Bone. 39 (2006) 505–512. doi:10.1016/j.bone.2006.02.074. [PubMed: 16679075]

[64]. Abbas S, Zhang Y-H, Clohisy JC, Abu-Amer Y, Tumor necrosis factor-α inhibits pre-osteoblast differentiation through its type-1 receptor, Cytokine. 22 (2003) 33–41. doi:10.1016/S1043-4666(03)00106-6. [PubMed: 12946103]

[65]. Meng F, Lowell CA, Lipopolysaccharide (LPS)-induced Macrophage Activation and Signal Transduction in the Absence of Src-Family Kinases Hck, Fgr, and Lyn, J. Exp. Med. 185 (1997) 1661–1670. doi:10.1084/jem.185.9.1661. [PubMed: 9151903]

[66]. Patil C, Zhu X, R. C Jr, Kim YJ, Kirkwood KL, p38 MAPK Regulates IL-1β Induced IL-6 Expression Through mRNA Stability in Osteoblasts, Immunol. Invest. 33 (2004) 213–233. doi:10.1081/IMM-120034231. [PubMed: 15195698]

[67]. Means TK, Pavlovich RP, Roca D, Vermeulen MW, Fenton MJ, Activation of TNF-alpha transcription utilizes distinct MAP kinase pathways in different macrophage populations., J. Leukoc. Biol. 67 (2000) 885–893. [PubMed: 10857863]

[68]. Yamane K, Ihn H, Asano Y, Jinnin M, Tamaki K, Antagonistic Effects of TNF-α on TGF-β Signaling Through Down-Regulation of TGF-β Receptor Type II in Human Dermal Fibroblasts, J. Immunol. 171 (2003) 3855–3862. doi:10.4049/jimmunol.171.7.3855. [PubMed: 14500687]

[69]. Wuu YD, Pampfer S, Vanderheyden I, Lee KH, De Hertogh R, Impact of tumor necrosis factor alpha on mouse embryonic stem cells, Biol. Reprod. 58 (1998) 1416–1424. [PubMed: 9623600]

Statement of Significance

Poly(ethylene glycol) (PEG)-based hydrogels are promising for cell encapsulation and tissue engineering, but are known to elicit a foreign body response (FBR) *in vivo*. The impact of the FBR on encapsulated cells and their ability to synthesize tissue has not been well studied. This study utilizes thiol-ene click chemistry to create a biomimetic, enzymatically degradable hydrogel system with which to encapsulate MC3T3-E1 pre-osteoblasts. The osteogenic capabilities and differentiation of these cells were studied in co-culture with macrophages, known drivers of the FBR. This study demonstrates that macrophages reduce osteogenic capabilities of encapsulated cells *in vitro* and suggest that the FBR should be considered for *in vivo* tissue engineering.

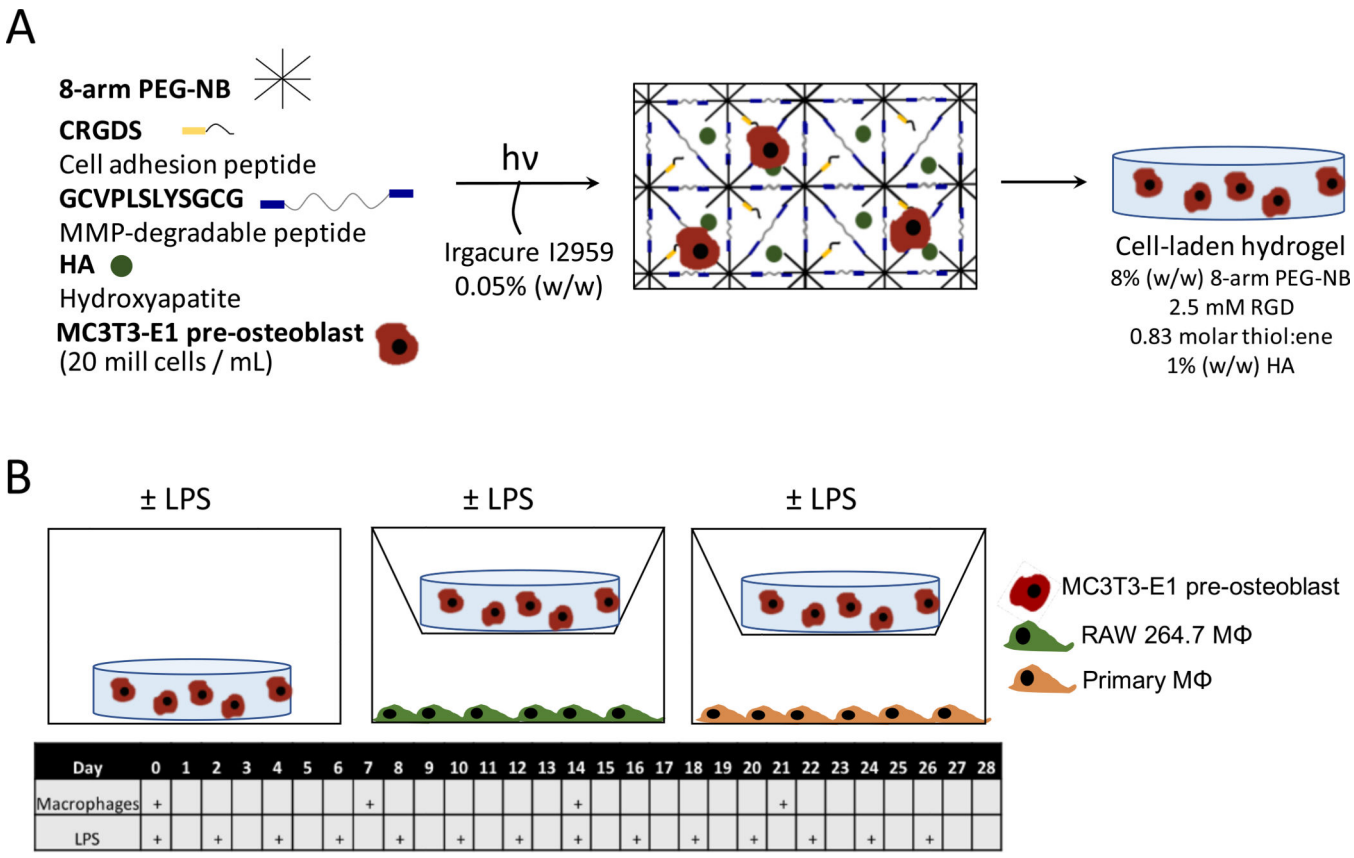

Figure 1 –.

Experimental setup. A) Schematic of the bone-mimetic hydrogel formation. B) Schematic of the experimental co-culture setup in this study, wherein macrophages were refreshed weekly and lipopolysaccharide (LPS) in the media was refreshed every 48 hours.

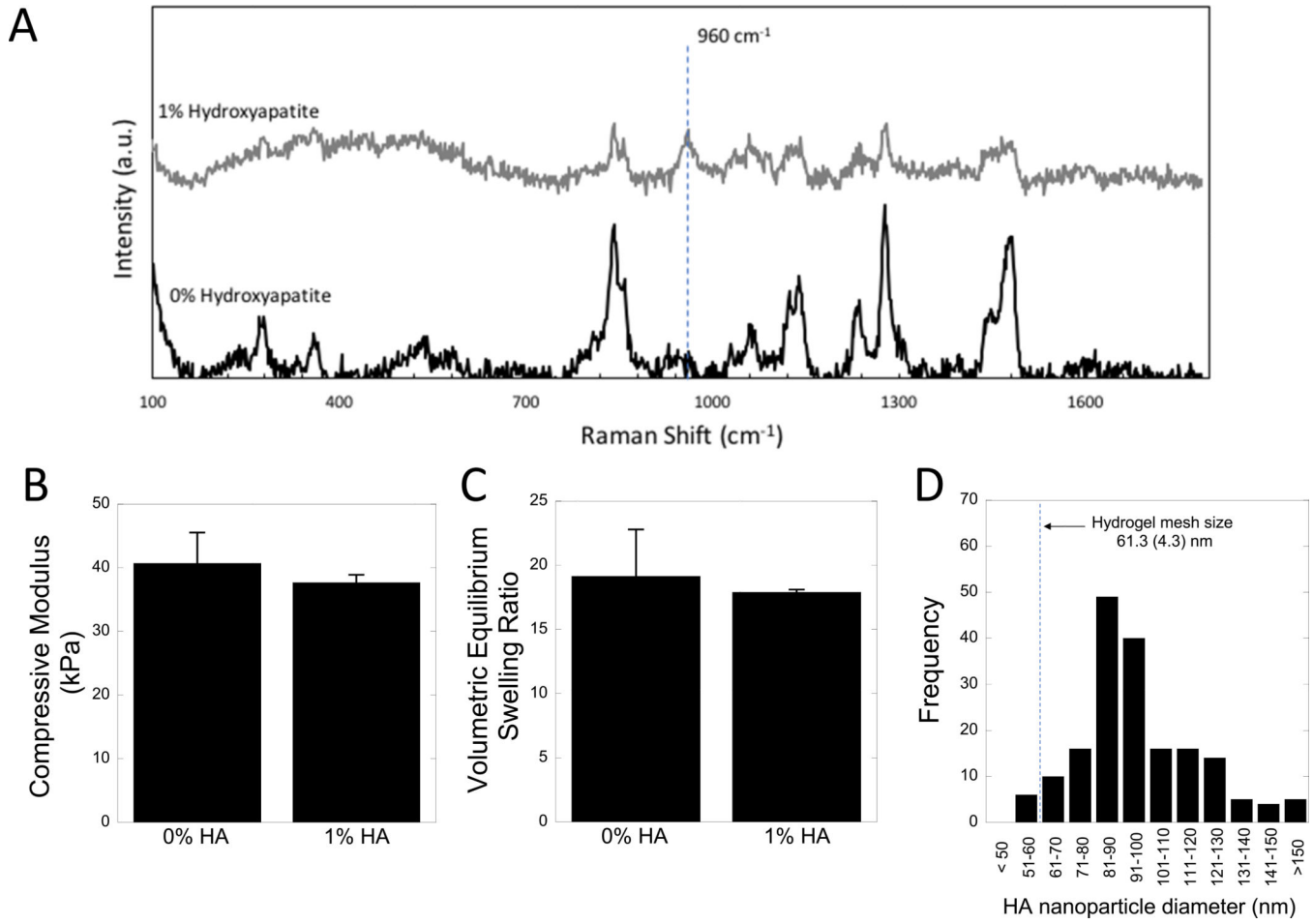

Figure 2 –.

Characterization of the acellular hydrogel. A) Raman spectroscopy of hydrogels with 0 and 1% hydroxyapatite (HA), showing the indicative hydroxyapatite peak at 960 cm^{-1}. B) Compressive modulus and C) volumetric equilibrium swelling ratio of hydrogels with 0 and 1% hydroxyapatite hydrogels. Data are shown as mean (n=3) with standard deviation as error bars. D) Histogram of hydroxyapatite nanoparticle diameter, determined by FESEM.

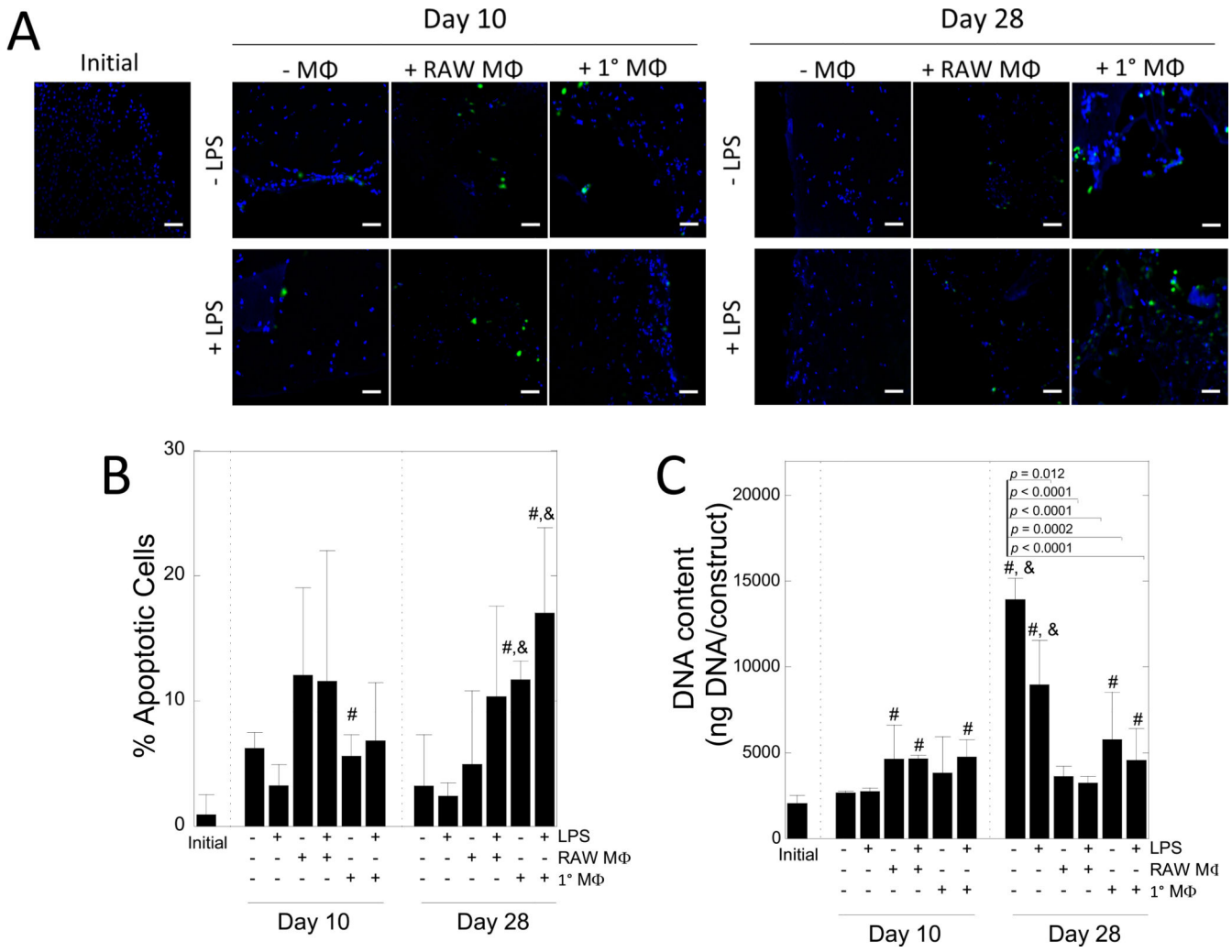

Figure 3 –.

The effects of macrophages on MC3T3-E1 cell apoptosis. A) Representative confocal microscopy images of hydrogels immediately after encapsulation and after 10 and 28 days of culture. Cells were stained for apoptosis (green) and counterstained with DAPI for cell nuclei (blue). Scale bar = 50 μm. B) Semi-quantification of the percent of apoptotic cells, normalized to number of nuclei in hydrogels after 0, 10, or 28 days of culture. C) DNA content per construct over time. Data are shown as mean (n=3–4) with standard deviation as error bars. "#" denotes statistical significance ($p < 0.05$) over day 0, "&" denotes statistical significance ($p < 0.05$) over day 10.

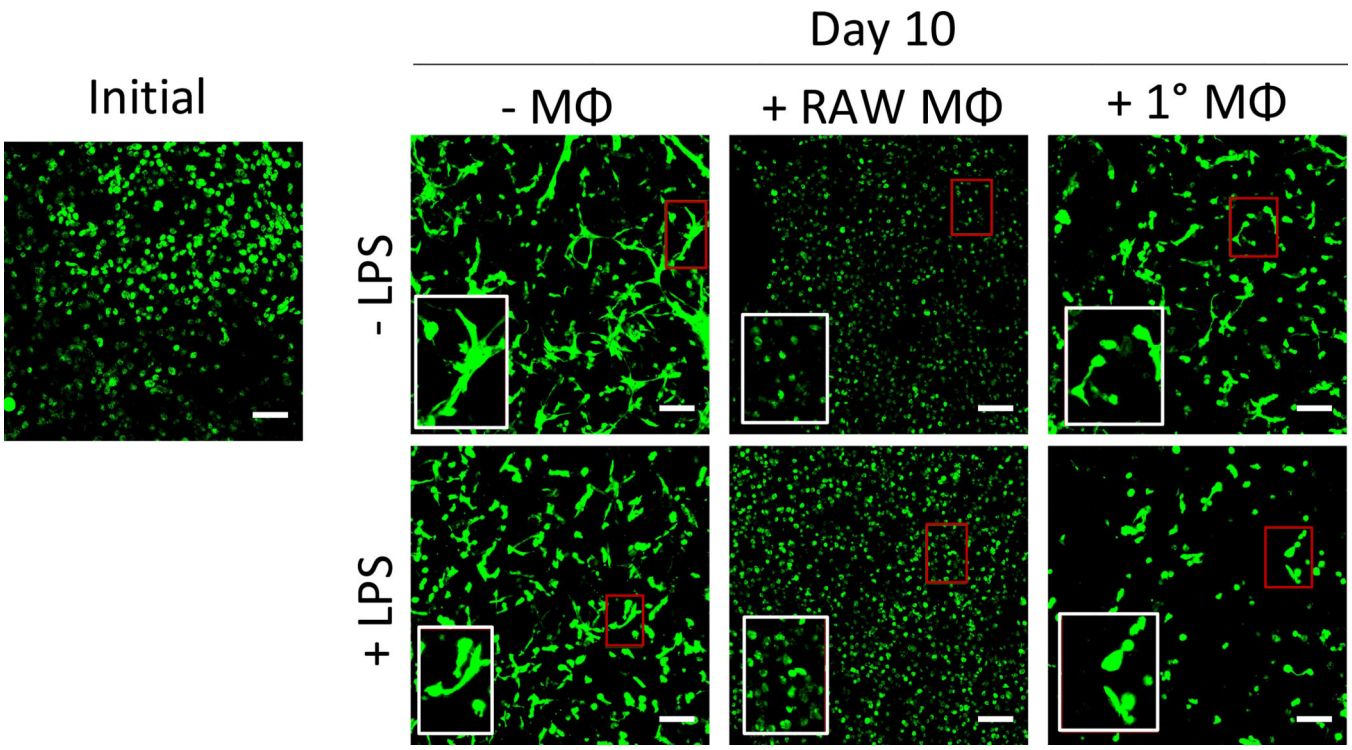

Figure 4 –.

The effects of macrophages on MC3T3-E1 cell morphology. Representative confocal microscopy images of hydrogels immediately after encapsulation and after 10 days of culture. Cells were stained using calcein AM to visualize morphology. Red box indicates region of interest, white box shows ROI at 2x magnification. Scale bar = 100 μm.

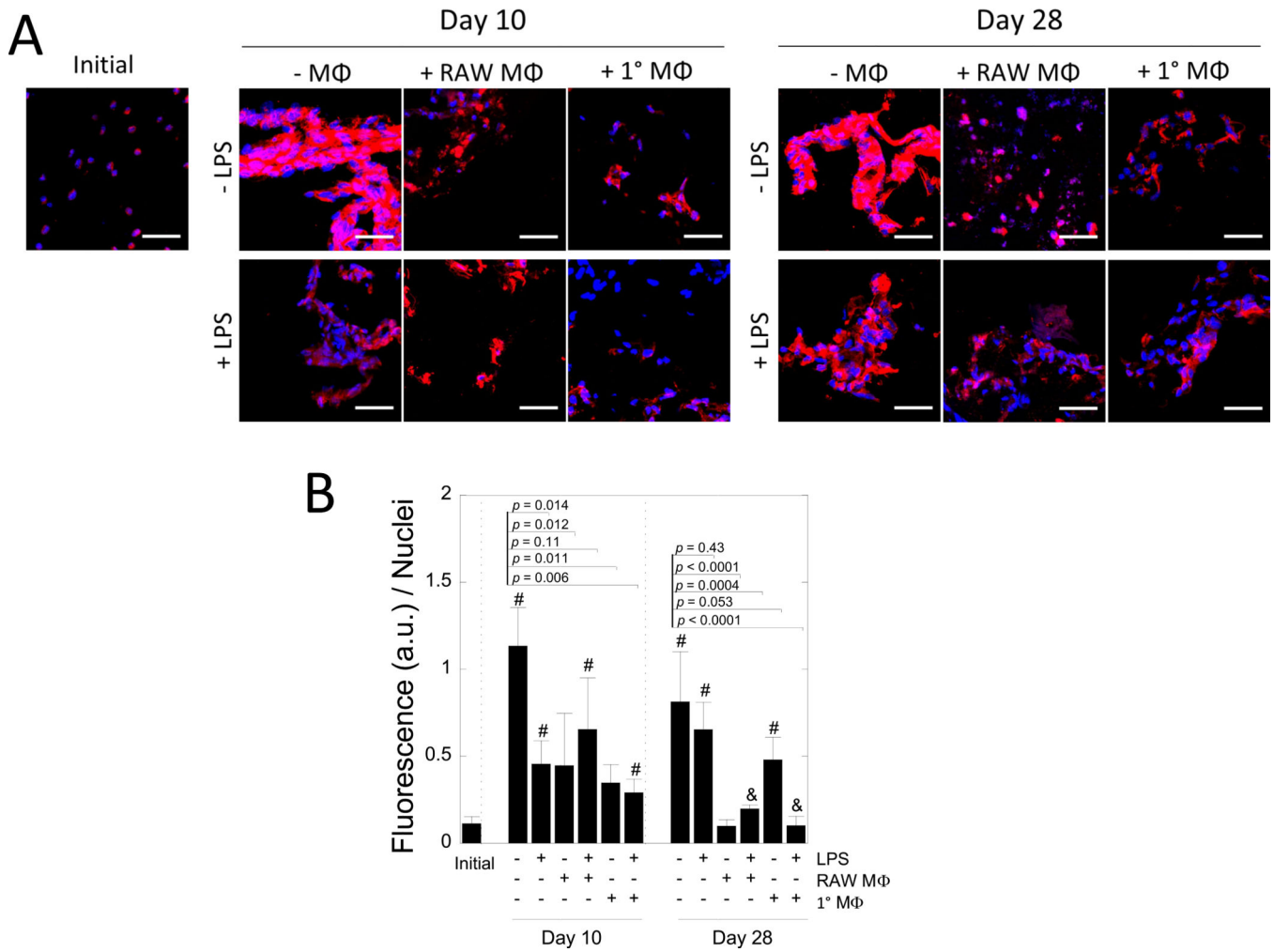

Figure 5 –.

The effect of macrophages on collagen I deposition by MC3T3-E1 cells. A) Representative confocal microscopy images of hydrogels after 0, 10, and 28 days of culture. Sections were stained for anti-collagen I (red) and counterstained with DAPI for cell nuclei (blue). Scale bar = 50 μm. B) Semi-quantification of the fluorescence (arbitrary units) normalized to the number of nuclei per image. Data are shown as mean (n=3–4) with standard deviation as error bars. P-values displayed are for pairwise comparisons between the unstimulated mono-culture and each treatment condition at each time point. "#" denotes statistical significance ($p < 0.05$) as compared to day 0, "&" denotes statistical significance ($p < 0.05$) as compared to corresponding condition at day 10.

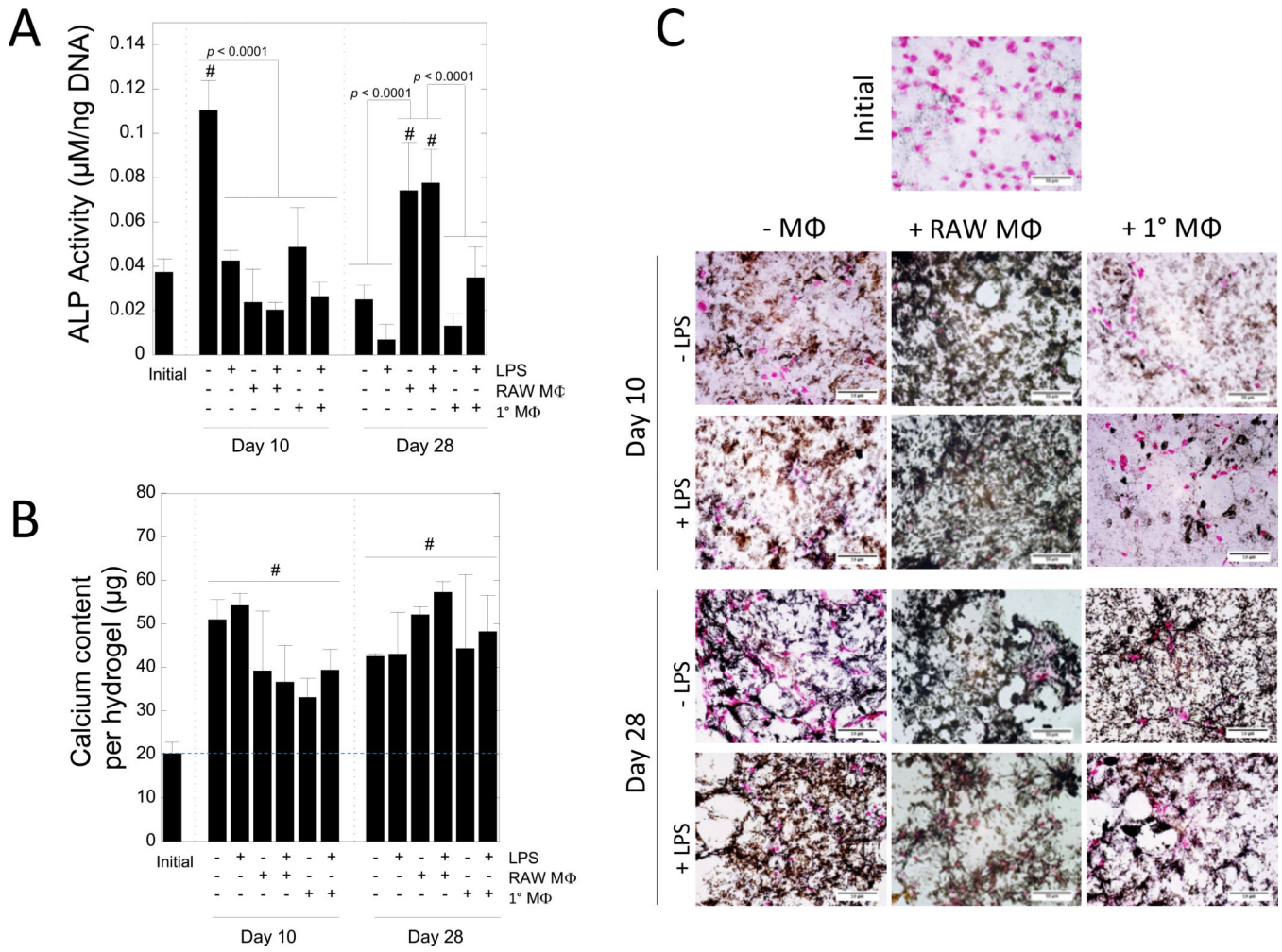

Figure 6 –.

The effects of macrophages on ALP activity and mineralization in MC3T3-E1-laden PEG hydrogels. A) ALP activity after 0, 10, and 28 days of culture. B) Total calcium content in hydrogels after 0, 10, and 28 days of culture. Blue dashed line indicates the mean calcium level at day 0, which provides a baseline for comparison. Data for A and B shown as mean (n = 3) with standard deviation as error bars. "#" denotes statistical significance ($p < 0.05$) as compared to day 0. C) Representative microscopy images of hydrogels fixed after 0, 10, and 28 days of culture and stained for von Kossa mineralization (black) and counterstained with nuclear fast red for nuclei (pink). Scale bar = 100 μm.

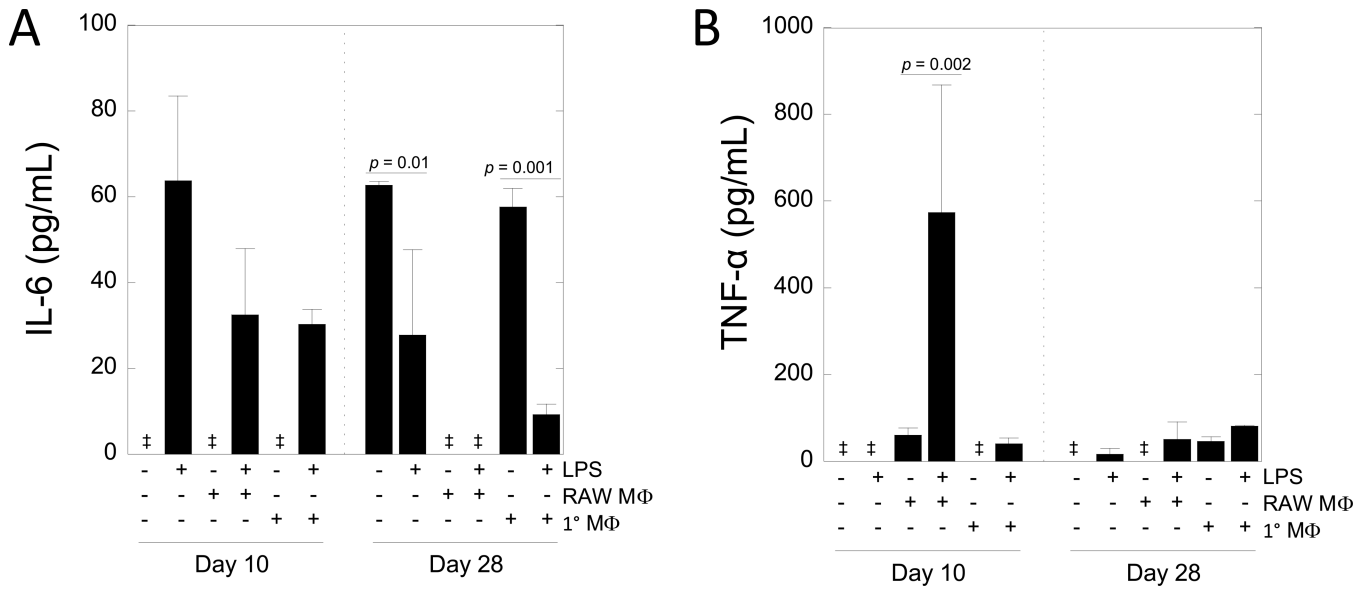

Figure 7 –.

Cytokine secretion from the in vitro co-culture model. A) Interleukin-6 (IL-6) and B) tumor necrosis factor alpha (TNF-a) secretion in the media on day 10 and 28 as assessed by enzyme-linked immunosorbent assay (ELISA). Data are shown as mean (n=3–4) with standard deviation as error bars. Double dagger denotes undetectable levels.

Table 1.

2-way ANOVA Statistical Analysis

2-way ANOVA Statistical Analysis

	Time	Treatment	Time*Treatment
TUNEL apoptosis	$p < 0.0001$	$p = 0.019$	$p = 0.014$
Collagen I	$p < 0.0001$	$p < 0.0001$	$p < 0.0001$
ALP activity	$p = 0.012$	$p < 0.0001$	$p < 0.0001$
Calcium content	$p < 0.0001$	$p = 0.943$	$p = 0.139$
IL-6	$p = 0.581$	$p = 0.095$	$p < 0.0001$
TNF-α	$p = 0.023$	$p < 0.0001$	$p < 0.0001$